Electronic Supplementary Information

Trimetallic PtNiCo branched nanocages as efficient and durable bifunctional electrocatalysts towards oxygen reduction and methanol oxidation reactions

Hengrui Ma, Zhiping Zheng, Hongsheng Zhao, Cong Shen, Hanming Chen, Huiqi Li, Zhenming Cao, Qin Kuang, Haixin Lin*, and Zhaoxiong Xie

State Key Laboratory for Physical Chemistry of Solid Surfaces, Collaborative, Innovation Center of Chemistry for Energy Materials Department of Chemistry College of Chemistry and Chemical Engineering, Xiamen University, Xiamen, 361005, China

* Email address: haixinlin@xmu.edu.cn

Supplemental Experimental Procedures

Chemicals and materials

Platinum (II) 2,4-pentanedionate ($Pt(acac)_2$, 99.4%), Cobalt (III) 2,4-pentanedionate ($Co(acac)_3$, 99%) and nickel (II) 2,4-pentanedionate ($Ni(acac)_2$, 95%) were purchased from Kunming Noble Metal Institute. Oleic acid ($C_{18}H_{34}O_2$, tech. 90%) and Pt/C (20 wt%) were purchased from Alfa Aesar. Formaldehyde solution (40%) and acetic acid (99.5%) were purchased from Sinopharm Chemical Reagent Co. Ltd. (Shanghai, China). Oleylamine ($C_{18}H_{37}N$) was purchased from J&K Chemicals.

Characterization

The morphology and crystal structure of products were observed by scanning electron microscopy (SEM, Hitachi S4800) and transmission electron microscopy (TEM, JEOL JEM 2100). High angle-annular dark-field scanning transmission electron microscopy (HAADF-STEM) was performed with a FEI TECNAI F30 microscope operating at 300 kV. The crystal structure of samples was determined by powder X-Ray diffraction (XRD) with a Rigaku Ultima IV diffractometer using Cu K_α radiation. Inductively coupled plasma mass spectrometry (ICP-MS, ThermoFisher iCAPQ) was employed to get precise elemental composition of samples, while X-ray photoelectron spectroscopy (XPS) was measured using a PHI Quantum-2000, with all spectra corrected based on the C1s peak (284.6 eV). The electrochemical tests were performed on an electrochemical workstation (CHI 760E, Shanghai Chenhua Co., China).

Experimental section

Synthesis of trimetallic PtNiCo nanomultipods

Trimetallic PtNiCo nanomultipods were prepared according to previously reported method with minor modification.[1] In a typical procedure, 8 mg $Pt(acac)_2$ (20 μmol), 11.8 mg $Ni(acac)_2$ (45 μmol) and 5.4 mg $Co(acac)_3$ (15 μmol) with molar ratio of 4:9:3 were dissolved in a mixed solvent of 9 mL of oleylamine and 1 mL of oleic acid. After the addition of 800 μL of the formaldehyde solution, the resulting solution was transferred into a 20 mL Teflon-lined stainless-steel autoclave reactor and heated at 220 °C for 12 hours. Trimetallic PtNiCo nanomultipods were obtained after centrifugation and washed with the mixture of ethanol and hexane for three times. For comparison, binary PtNi nanomultipods were synthesized in the absence of $Co(acac)_3$ in an otherwise analogous process.

Synthesis of PtNiCo branched nanocages

The as-prepared PtNiCo nanomultipods were immersed in 15 mL of acetic acid and heated at 70 °C for 12 h. Following this, the products (denoted as *h*-PtNiCo) were collected and washed with ethanol three times. Hollow PtNi nanomultipods (denoted as *h*-PtNi) was synthesized using the same acid etching process from PtNi nanomultipods.

Electrochemical measurements of samples

Before electrochemical measurements, the PtNiCo or PtNi catalysts were supported with Vulcan XC-72 carbon powder (denoted as *h*-PtNiCo/C and *h*-PtNi/C, respectively), which was dispersed, along with the catalysts, in a solvent of isopropanol and Nafion (5 wt%) ($V_{isopropanol}$: V_{Nafion} = 100:1) and ultrasonically mixed for 3 hours to form a catalyst ink (2 mg mL^{-1}). All the electrochemical measurements were conducted in a three-electrode cell where a saturated

calomel electrode (SCE) and a carbon rod were used as reference and counter electrodes, respectively.

For ORR tests, a glassy carbon rotating disk electrode (RDE) (5 mm in diameter) was loaded with catalyst and served as the working electrode. Pt loadings for *h*-PtNiCo/C, *h*-PtNi/C, and Pt/C were 3.4, 3.5 and 4.0 μg respectively, as measured by ICP-MS. Cyclic voltammograms (CVs) were firstly conducted in a N_2-saturated $HClO_4$ solution at a rotation speed of 1600 rpm, between 0.05−1.05 V (versus RHE) at a scanning rate of 50 mV s^{-1}. The electrochemically active surface area (ECSA) of catalysts were determined by the area of the hydrogen desorption peaks in the CV measurement. After the CV curve stabilized, ORR tests were carried out in an O_2-saturated 0.1 M $HClO_4$ solution. The linear sweep voltammetry (LSV) was performed at a scan rate of 10 mV s^{-1} and a rotation speed of 1600 rpm. All the LSV curves were corrected by 85% iR drop compensation. The kinetic current (i_k) at 0.9 V (versus RHE) was calculated by the Koutecky-Levich equation ($1/i = 1/i_k + 1/i_L$) to study the mass and specific activities. An accelerated durability test (ADT) was recorded in the O_2-saturated 0.1 M $HClO_4$ solution between 0.6-1.1 V (versus RHE) at a scanning rate of 100 mV s^{-1}.

In MOR tests, a glassy carbon electrode (3 mm in diameter) served as working electrode, with Pt loadings of 2.8, 2.8, and 3.0 μg for *h*-PtNiCo/C, *h*-PtNi/C, and Pt/C, respectively, as measured by ICP-MS. MOR tests were performed in a solution of 0.1 M $HClO_4$ + 0.5 M CH_3OH at a scan rate of 50 mV s^{-1}. The specific activities of catalysts were normalized by their ECSAs. For the CO-stripping experiments, CO was purged into the 0.1 M $HClO_4$ solution for 15 min, and then N_2 was purged to remove dissolved CO before striping curves were measured at a scan

rate of 10 mV s^{-1} between 0.05−1.2 V (versus RHE).

Electrochemical *in situ* FTIR spectroscopy

Electrochemical *in situ* Fourier transform infrared (FTIR) spectroscopic experiments were carried out on a Nexus 870 FTIR (Nicolet) which is equipped with a liquid-nitrogen-cooled MCT-A detector, an EverGlo IR source and at a spectral resolution of 8 cm^{-1}. And infrared radiation sequentially passed through a CaF_2 window and a thin-layer solution (about 10 μm), and then it was reflected by the electrode surface. And the final resulting spectra were reported as a relative change which were defined as the following equation:

$$\frac{\Delta R}{R} = \frac{R(E_s) - R(E_R)}{R(E_R)}$$

Herein, R(E_S) and R(E_R) are the single-beam spectra collected at sample potential E_S and the reference potential E_R, respectively. In this experiment for MOR tests, the E_R is 0 V (versus SCE), at which the methanol cannot be oxidized; and the *in situ* CO adsorption experiment, the E_R is 1.0 V (versus SCE), at which the adsorbed CO is oxidized completely.

Results and discussion

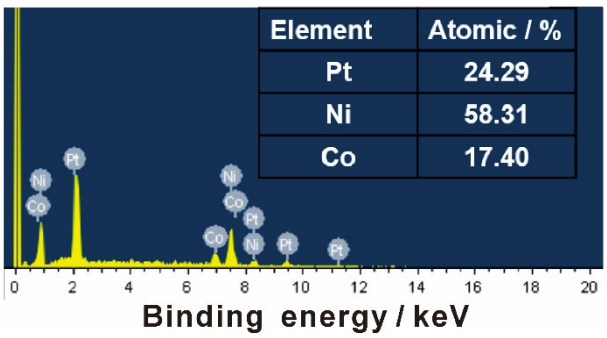

Figure S1. EDS analysis of PtNiCo nanomultipods.

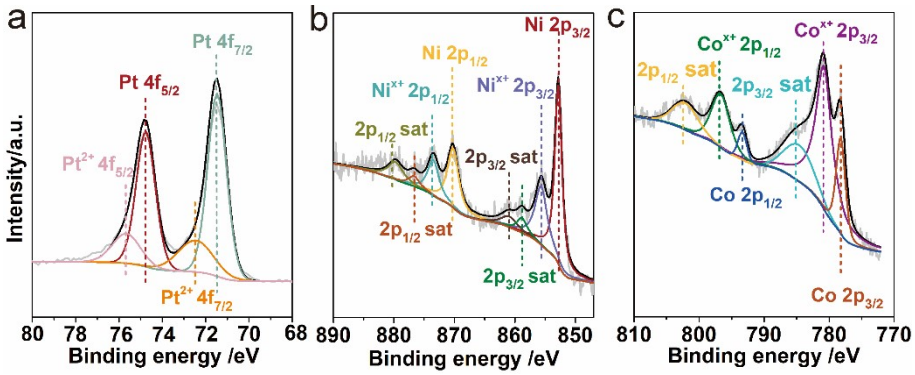

Figure S2. XPS characterization of (a) Pt 4f, (b) Ni 2p, (c) Co 2p of PtNiCo nanomultipods.

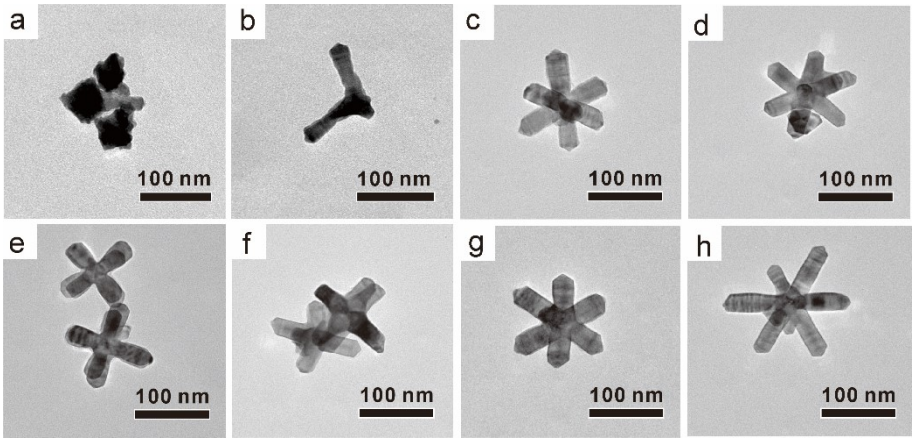

Figure S3. TEM images of PtNiCo nanomultipods collected at different reaction times: (a) 20 min, (b) 40 min, (c) 1 h, (d) 2 h, (e) 3 h, (f) 6 h, (g) 9 h, (h) 12 h.

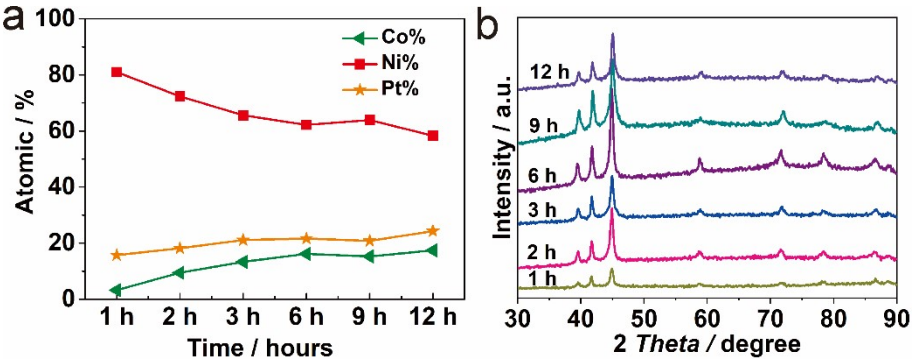

Figure S4. (a) EDS element contents and (b) XRD patterns of PtNiCo nanomultipods collected at different reaction times.

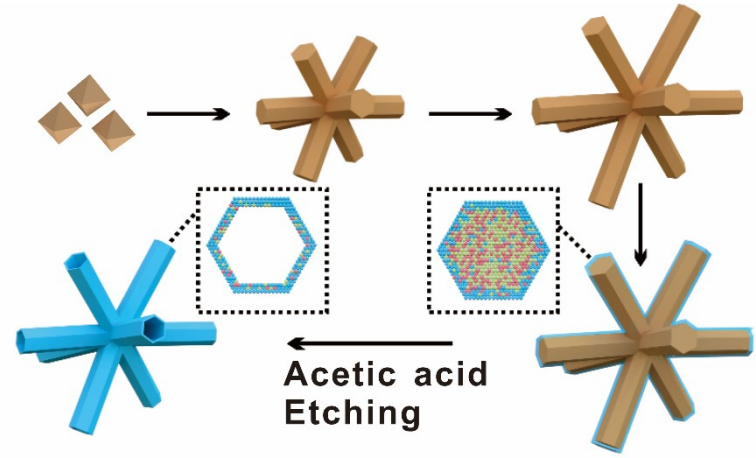

Figure S5. Schematic illustration of the formation of PtNiCo branched nanocages.

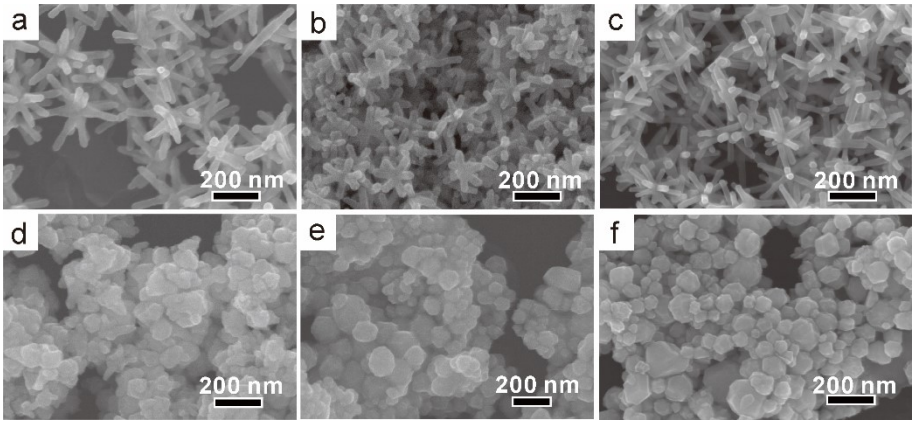

Figure S6. SEM images of products obtained with different molar ratios of precursors, the molar ratio of $Pt(acac)_2$ is three time of the total molar ratio of $Ni(acac)_2$ and $Co(acac)_3$, and just the $Ni(acac)_2$:$Co(acac)_3$ value was changed. (a) $Ni(acac)_2$:$Co(acac)_3$=1:0, (b) $Ni(acac)_2$:$Co(acac)_3$=5:1, (c) $Ni(acac)_2$:$Co(acac)_3$=3:1, (d) $Ni(acac)_2$:$Co(acac)_3$=1:1, (e) $Ni(acac)_2$:$Co(acac)_3$=1:3, (f) $Ni(acac)_2$:$Co(acac)_3$=0:1.

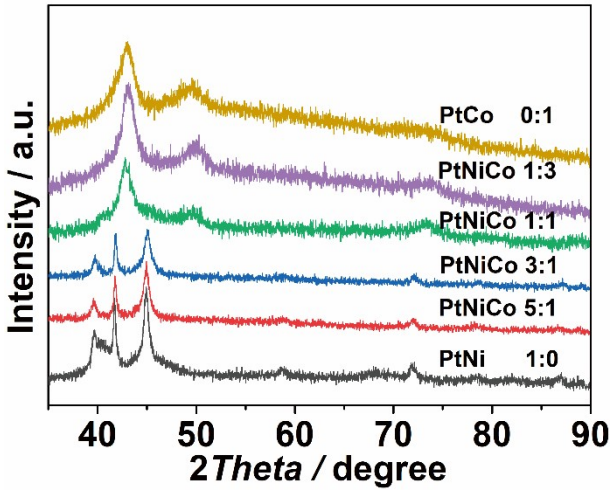

Figure S7. XRD patterns of products obtained with different molar ratios of precursors.

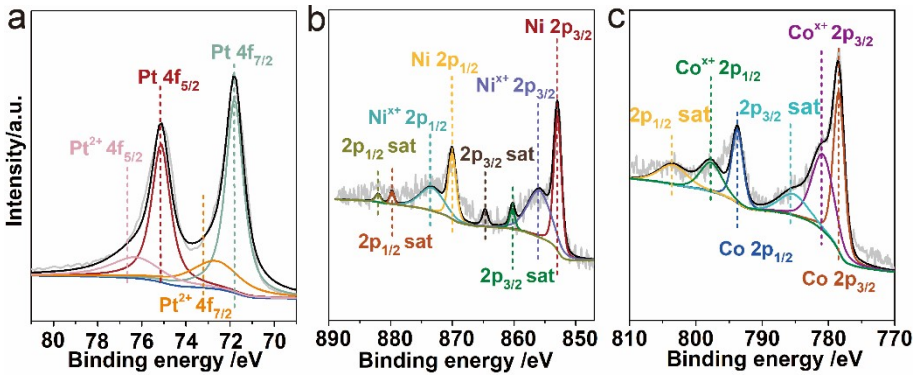

Figure S8. XPS characterization of (a) Pt 4f, (b) Ni 2p, (c) Co 2p of PtNiCo branched nanocages.

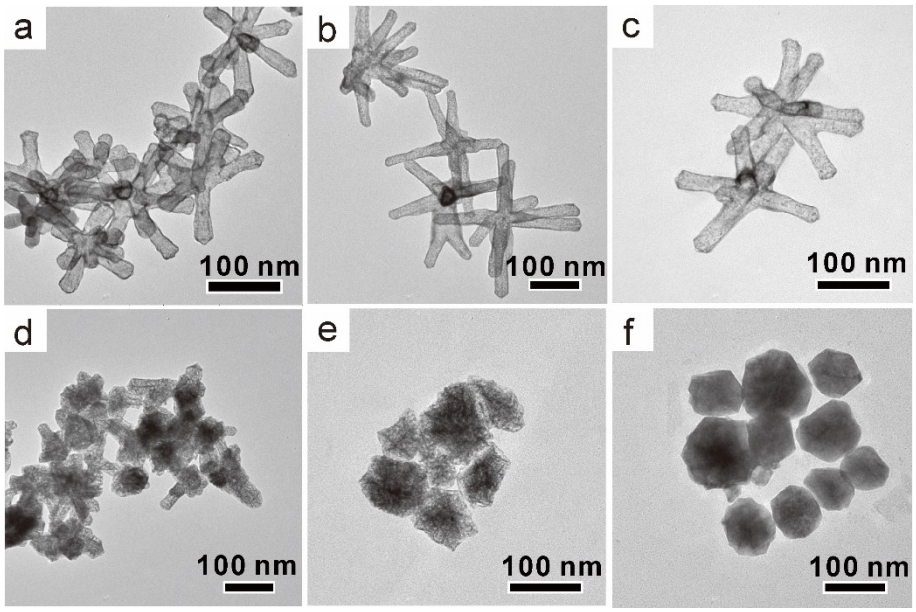

Figure S9. TEM images of the acetic acid-etched products obtained with different molar ratios of precursors. (a) $Ni(acac)_2$:$Co(acac)_3$=1:0, (b) $Ni(acac)_2$:$Co(acac)_3$=5:1, (c) $Ni(acac)_2$:$Co(acac)_3$=3:1, (d) $Ni(acac)_2$:$Co(acac)_3$=1:1, (e) $Ni(acac)_2$:$Co(acac)_3$=1:3, (f) $Ni(acac)_2$:$Co(acac)_3$=0:1.

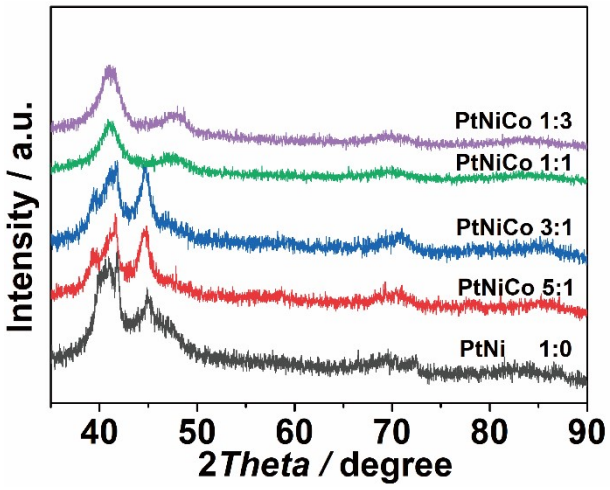

Figure S10. XRD patterns of the acetic acid-etched products obtained with different molar ratios of precursors.

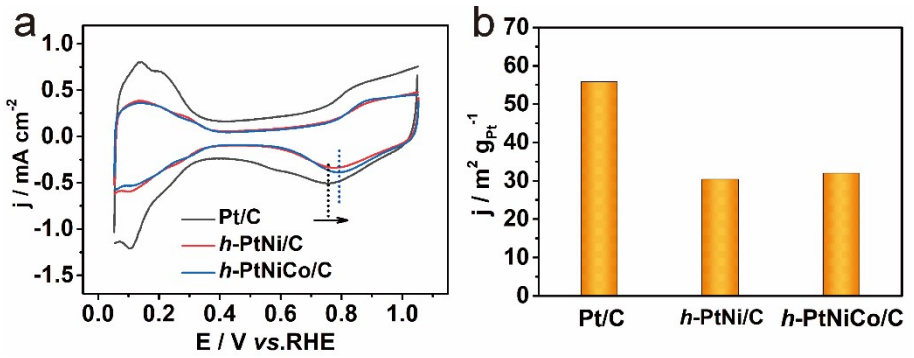

Figure S11. (a) CV curves of different catalysts in 0.1 M $HClO_4$ with a scan rate of 50 mVs^{-1}. (b) The $ECSA_H$ of different catalysts.

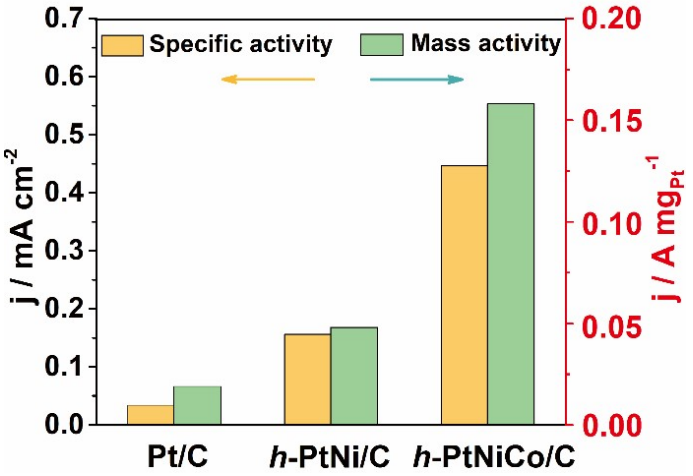

Figure S12. The comparison of specific activity and mass activity of different catalysts for ORR at 0.95 V (vs. RHE).

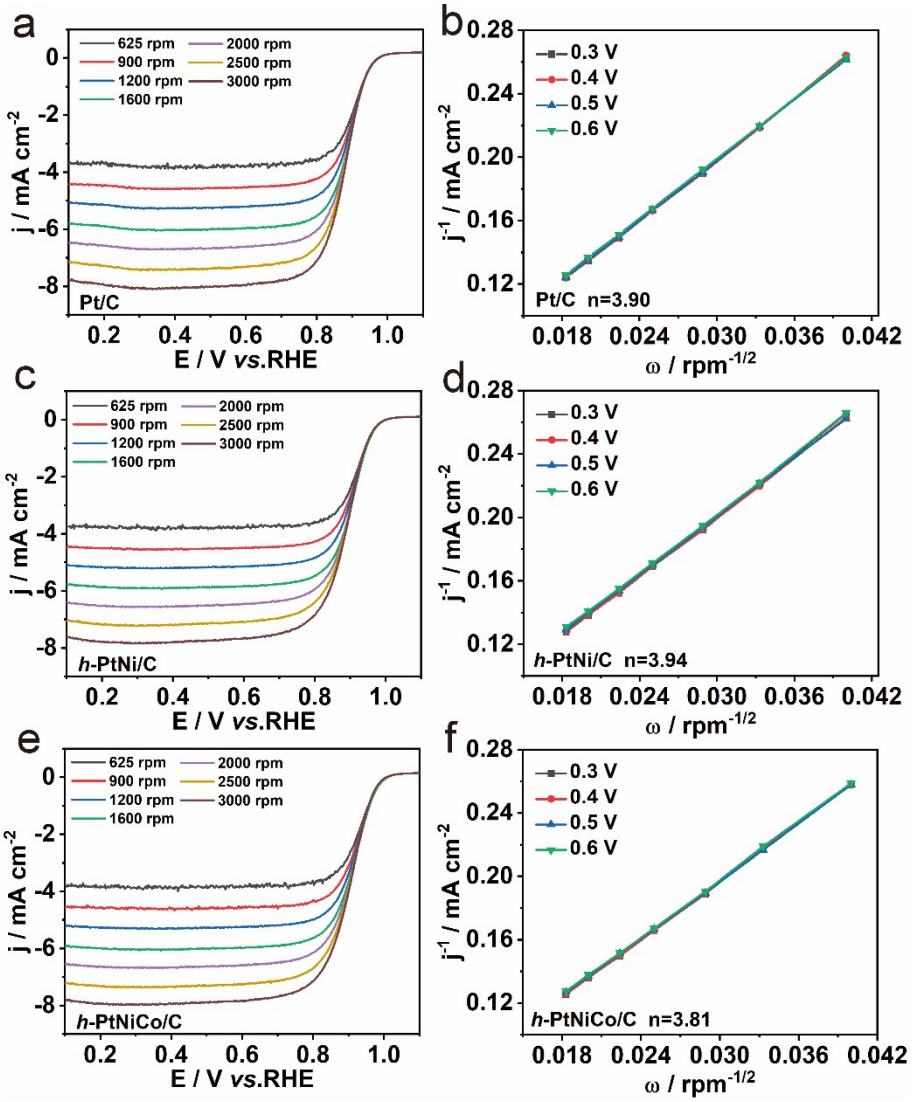

Figure S13. ORR polarization curves at different rotation rates and corresponding K-L plots: (a-b) Pt/C, (c-d) *h*-PtNi/C, (e-f) *h*-PtNiCo/C.

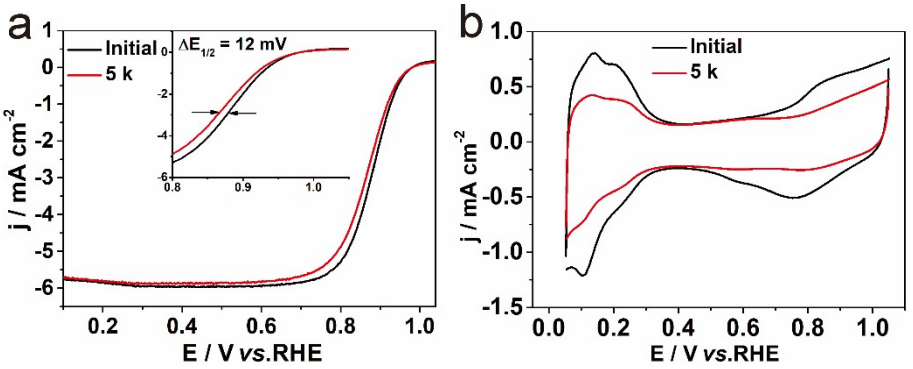

Figure S14. (a) LSV curves of Pt/C before and after 5,000 cycles of durability test in 0.1 M $HClO_4$ solution at a scanning rate of 10 mV s^{-1}, (b) CV curves of Pt/C before and after 5,000 cycles of durability test at a scanning rate of 10 mV s^{-1}.

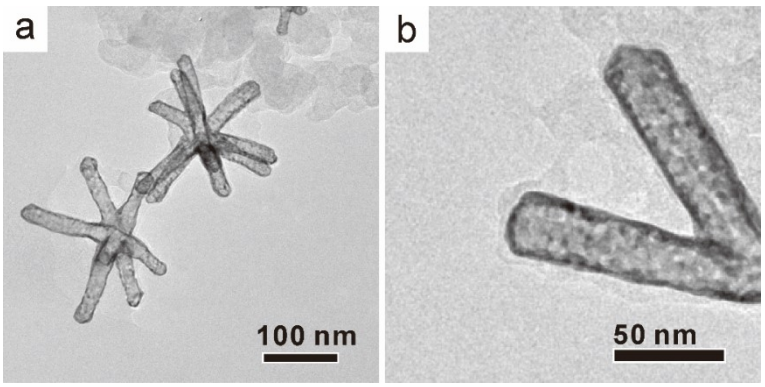

Figure S15. TEM images of *h*-PtNiCo/C after 10,000 cycles ORR durability test: (a) *h*-PtNiCo/C naocages, (b) a single branch of *h*-PtNiCo/C nanocage.

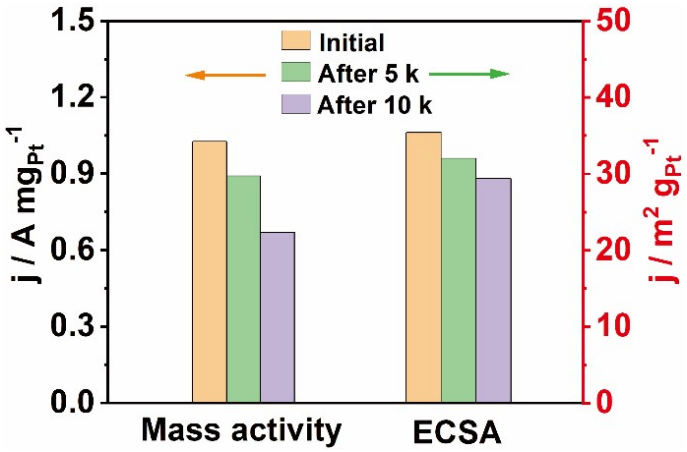

Figure S16. The mass activity (at 0.9 V versus RHE) and ECSA of *h*-PtNiCo/C before and after different cycles of durability test.

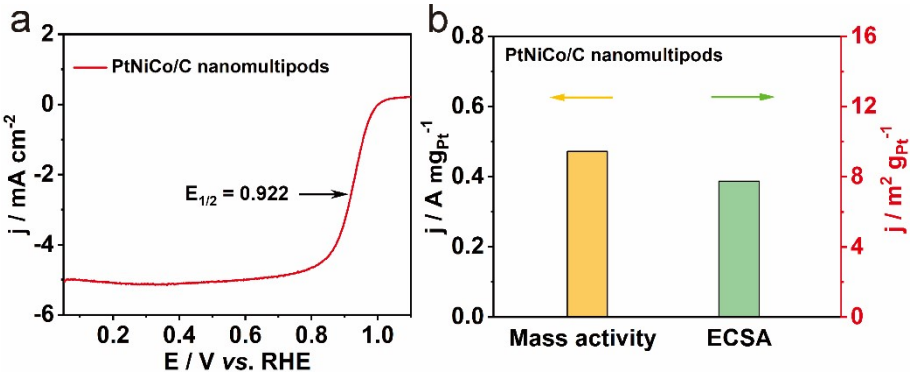

Figure S17. ORR performance for PtNiCo/C nanomultipods: (a) LSV curves recorded in O_2-saturated 0.1 M $HClO_4$ solution at a scan rate of 10 mV s^{-1} and 1600 rpm rotation rate; (b) mass activity and $ECSA_H$.

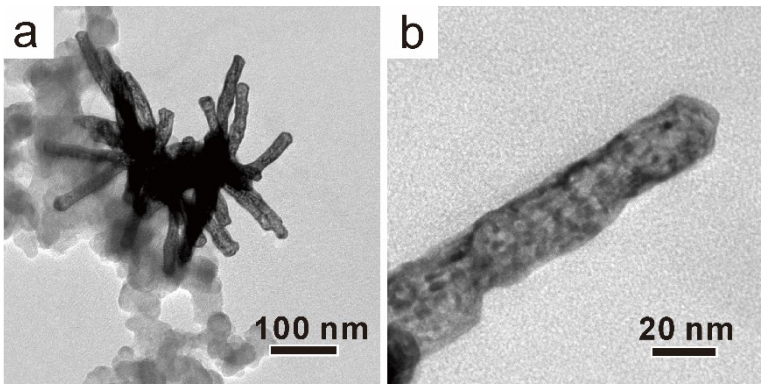

Figure S18. TEM images of PtNiCo/C nanomultipods after ORR test: (a) PtNiCo/C nanomultipods, (b) a single branch of PtNiCo/C nanomultipod.

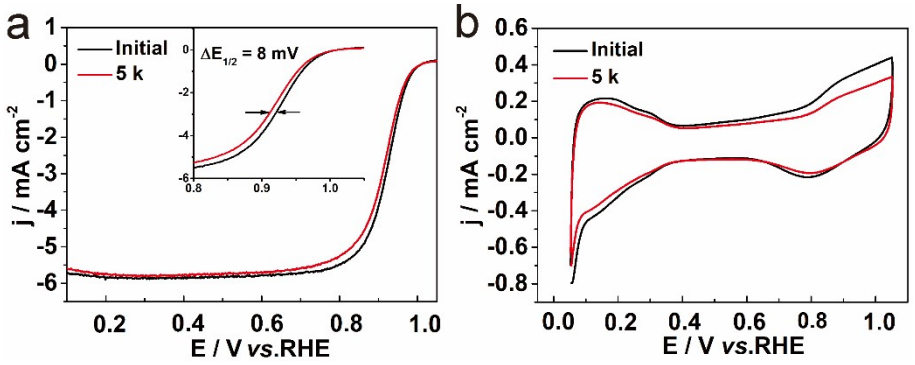

Figure S19. (a) LSV curves of electrochemically etched *EC*-PtNiCo/C before and after 5,000 cycles of durability test in 0.1 M $HClO_4$ solution at a scanning rate of 10 mV s^{-1}, (b) CV curves of electrochemical etched *EC*-PtNiCo/C before and after 5,000 cycles of durability test at a scanning rate of 50 mV s^{-1}.

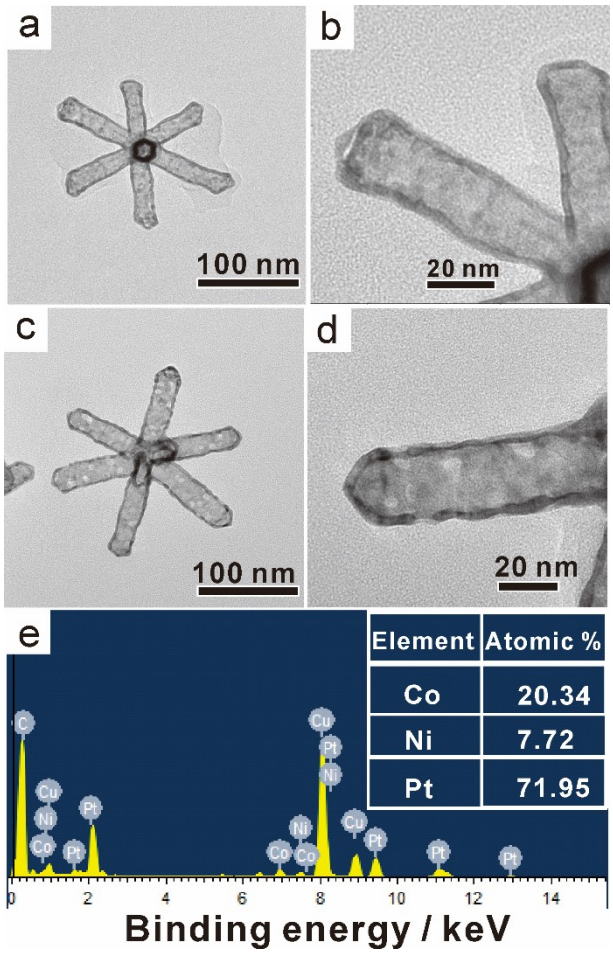

Figure S20. Characterization of electrochemically etched *EC*-PtNiCo/C before and after 5,000 cycles of durability test: (a-b) TEM images of *EC*-PtNiCo/C before durability test, (c-d) TEM images of of *EC*-PtNiCo/C after 5,000 cycles of durability test, (e) EDX analysis of *EC*-PtNiCo/C after 5,000 cycles of durability test.

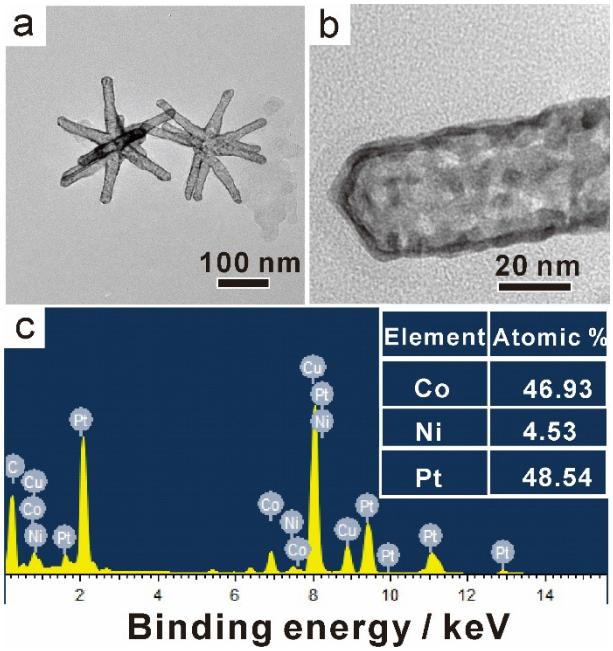

Figure S21. Characterization of acetic etched *h*-PtNiCo/C after 5,000 cycles of durability test:

(a) TEM image, (b) TEM image of a single branch, (c) EDX analysis.

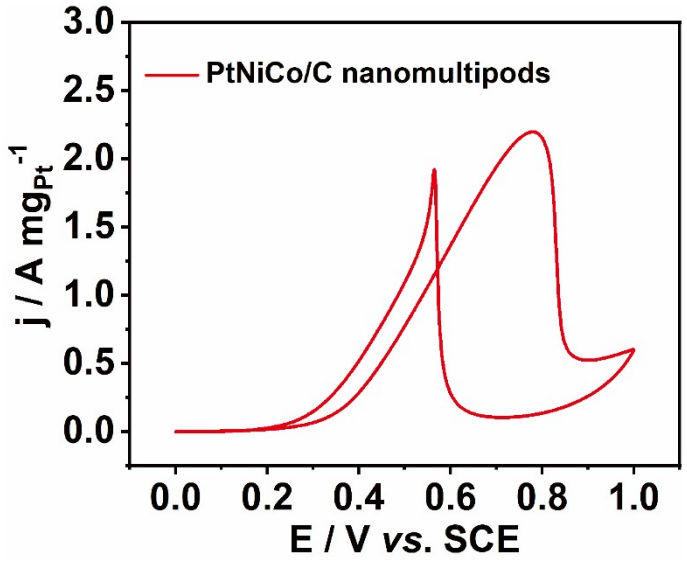

Figure S22. MOR performance of PtNiCo/C nanomultipods normalized by Pt loading in 0.1 M $HClO_4$ and 0.5 M CH_3OH at a scan rate of 50 mV s^{-1}

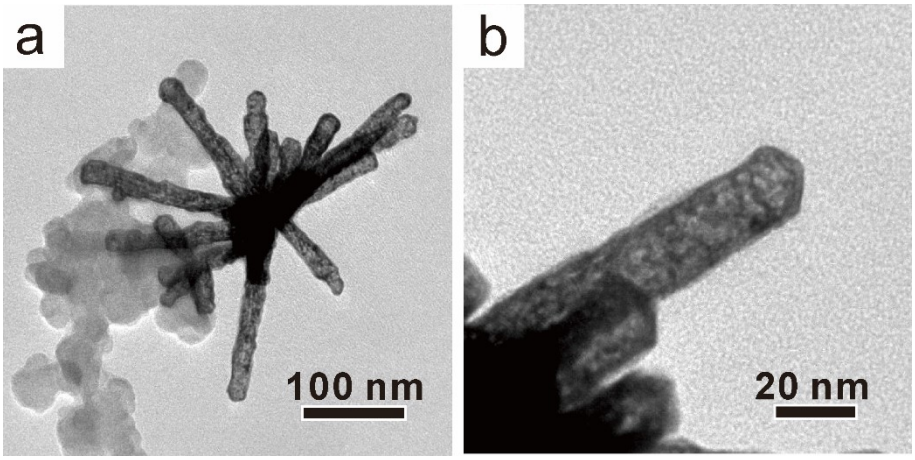

Figure S23. TEM images of PtNiCo/C nanomultipods after MOR test: (a) PtNiCo/C nanomultipods, (b) a single branch of PtNiCo/C nanomultipod.

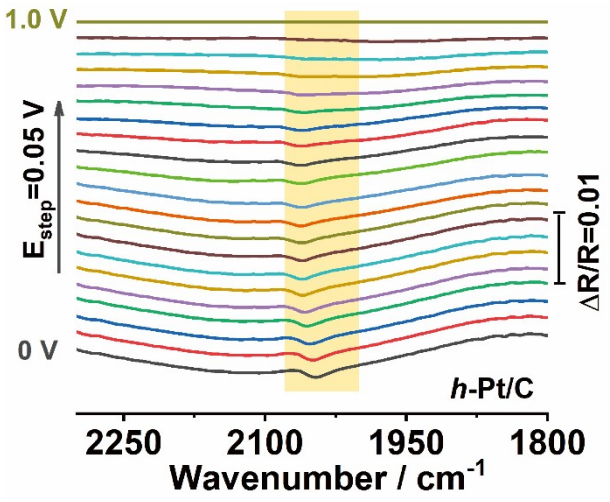

Figure S24. *In situ* FTIR spectra of MOR for Pt/C, E_s = 0-1.0 V, E_R = 1.0 V, E_{step} = 0.05 V.

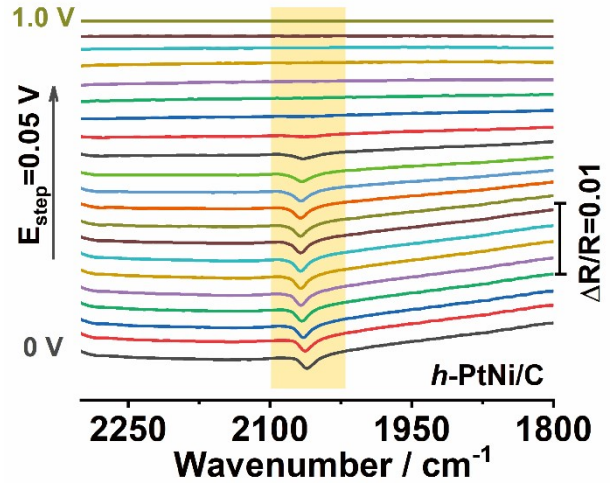

Figure S25. *In situ* FTIR spectra of MOR for *h*-PtNi/C, E_s = 0-1.0 V, E_R = 1.0 V, E_{step} = 0.05 V.

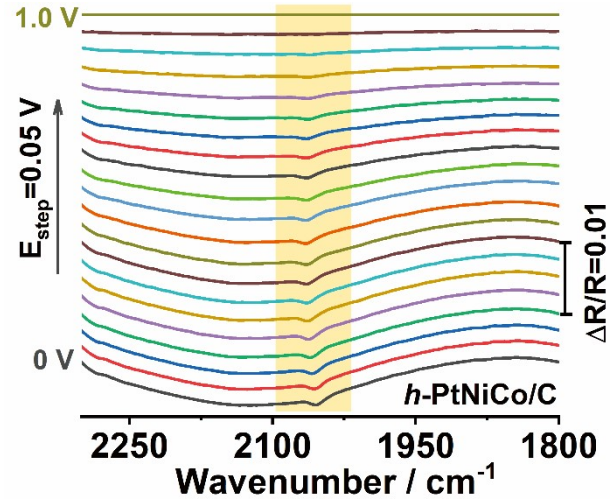

Figure S26. *In situ* FTIR spectra of MOR for *h*-PtNiCo/C, E_s = 0-1.0 V, E_R = 1.0 V, E_{step} = 0.05 V.

Table S1. Summary of the ORR performance of Pt-based catalysts reported in recent years.

Catalyst	Mass activity ($A \cdot mg_{Pt}^{-1}$)	Specific Activity ($mA \cdot cm^{-2}$)	Reference
***h*-PtNiCo branched nanocages**	**1.03**	**2.75**	**This work**
Pd/PtFe core/shell nanotubes	2.71	4.32	*Science Bulletin* 2021, **66**, 44–51.
Au@Co@PtCoAu	0.69	1.73	*Adv. Funct. Mater.* 2020, **30**, 2001575.
$L1_0$-PtZn	1.02	1.68	*Adv. Energy Mater.* 2020, **10**, 2000179.
$Pt_2CuW_{0.25}/C$	0.75	1.43	*Adv. Funct. Mater.* 2020, **30**, 1908230.
PtFe twisty nanowire	3.40	3.50	*J. Am. Chem. Soc.* 2020, **142**, 1287-1299.
Pt_3In Clusters	0.71	0.91	*Adv. Sci.* 2020, **7**, 1901279.
Hollow PtFe alloy nanoparticles	1.02	2.73	*Chem. Eur. J.* 2020, **26**, 4090 – 4096.
$L1_0$-Pt-Ni-Co	2.28	4.38	*Adv. Energy Mater.* 2019, **9**, 1803771.
Sub-2 nm Pt Particles	0.75	0.32	*Nano Lett.* 2019, **19**, 4997-5002.
$L1_0$-W-PtCo/C	2.21	3.60	*Angew. Chem. Int. Ed.* 2019, **58**, 15471-15477.
PtCuNi Nanoframe	0.86	1.65	*J. Power Sources* 2018, **406**, 42-49.
$Fe_3Pt/Ti_{0.5}Cr_{0.5}N$	0.64	1.28	*Adv. Energy Mater.* 2019, **9**, 1803040.
Pt–Cu Nanoparticles	0.48	0.53	*ACS Appl. Mater. Interfaces* 2017, **9**, 35740-35748.
Excavated octahedral Pt-Co	0.39	2.41	*Nano Energy* 2017, **39**, 582–589.
Pd@Pt octahedral nanocages	0.75	1.98	*Science* 2015, ***349***, 412-416.
Pt_3Ni Nanoframes	5.7	~1.95 (at 0.95V versus RHE)	*Science* 2014, ***343***, 1339-1343.

Table S2. Summary of the MOR performance of Pt-based catalysts reported in recent years.

Catalyst	Mass activity ($A \cdot mg_{Pt}^{-1}$)	Specific Activity ($mA \cdot cm^{-2}$)	Condition	Reference
_h_-PtNiCo branched nanocages	**2.82**	**5.73**	**0.1 M $HClO_4$ + 0.5 M CH_3OH**	**This work**
Pd/PtFe core/shell nanotubes	2.68	4.27	0.1 M $HClO_4$ + 0.5 M CH_3OH	*Science Bulletin* 2021, **66**, 44–51.
PtCo@NCs	2.3	5.14	0.1 M $HClO_4$ + 1.0 M CH_3OH	*Adv. Funct. Mater.* 2020, **30**, 2002281.
PtCoNiRh nanowires	1.36	2.08	0.1 M $HClO_4$ + 0.5 M CH_3OH	*Nano Energy* 2020, **71**, 104623.
Ce-modified Pt nanoparticle	1.47	1.20	0.5 M H_2SO_4 + 1.0 M CH_3OH	*Nano Energy* 2020, **71**, 104784.
Hollow Pt-Ni-Co Nanodendrites	2.20	3.8	0.5 M H_2SO_4 + 1.0 M CH_3OH	*ACS Appl. Energy Mater.* 2019, **2**, 961-965.
PtPdAg Hollow Nanodendrites	1.58	3.75	0.1 M $HClO_4$ + 0.2 M CH_3OH	*Small Methods* 2019, **4** 1900709.
PtSn intermetallic Nanoparticles	1.52	6.09	0.5 M H_2SO_4 + 1.0 M CH_3OH	*Nanoscale* 2019, **11** 19895-19902.
Sierpinski gasket octahedron-like PtAg	0.73	6.61	0.1 M $HClO_4$ + 0.5 M CH_3OH	*Nano Energy* 2019, **61**, 397-403.
Hexapod PtRuCu Nanocrystalline	1.35	5.22	0.1 M $HClO_4$ + 1 M CH_3OH	*ACS Catal.* 2018, **8**, 7578-7584.
PtRu Nanowires	0.82	1.16	0.1 M $HClO_4$ + 0.5 M CH_3OH	*J. Am. Chem. Soc.* 2018, **140**, 1142-1147.
Excavated octahedral Pt-Co	0.52	2.57	0.5 M H_2SO_4 + 0.5 M CH_3OH	*Nano Energy* 2017, **39**, 582-589.
Excavated Pt_3Co Nanocubes	0.65	4.14	0.5 M H_2SO_4 + 1.0 M CH_3OH	*Chem. Mater.* 2017, **29**, 9613-9617.
PtCu nanotubes	2.25	6.09	0.5 M H_2SO_4 + 1.0 M CH_3OH	*Energy Environ. Sci.* 2017, **10**, 1751-1756.
Excavated cubic Pt-Sn Nanocrystals	0.35	2.30	0.5 M H_2SO_4 + 0.5 M CH_3OH	*Angew. Chem. Int. Ed.* 2016, **55**, 9021-9025.
Mesoporous Pt Nanoparticles	0.41	1.29	0.1 M $HClO_4$ + 0.5 M CH_3OH	*Angew. Chem. Int. Ed.* 2016, **55**, 10037-10041.

Reference

1. Z. Cao, H. Li, C. Zhan, J. Zhang, W. Wang, B. Xu, F. Lu, Y. Jiang, Z. Xie and L. Zheng,

Nanoscale, 2018, **10**, 5072-5077.